Contents lists available at ScienceDirect

Pattern Recognition

journal homepage: www.elsevier.com/locate/pr

Human identification by quantifying similarity and dissimilarity in electrocardiogram phase space

Shih-Chin Fang[a,b], Hsiao-Lung Chan[a,*]

[a]Department of Electrical Engineering, Chang Gung University, 259 Wenhwa 1st Road, Kweishan, Taoyuan 333, Taiwan
[b]Department of Neurology, Cardinal Tien Hospital Yung Ho Branch, Taipei, Taiwan

ARTICLE INFO

Article history:
Received 24 February 2008
Received in revised form 9 November 2008
Accepted 20 November 2008

Keywords:
Biometrics
Human identification
Electrocardiogram (ECG)
Phase space reconstruction
Unsupervised classification

ABSTRACT

Specific patterns of electrocardiogram (ECG), along with other biometrics, have recently been used to recognize a person. Most ECG-based human identification methods rely on the reduced features derived from ECG characteristic points and supervised classification. However, detecting characteristic points is an arduous procedure, particularly at low signal-to-noise ratios. The supervised classifier requires retraining when a new person is included in the group. In the present study, we propose a novel unsupervised ECG-based identification method based on phase space reconstruction of one-lead or three-lead ECG, saving from picking up characteristic points. Identification is performed by inspecting similarity or dissimilarity measure between ECG phase space portraits. Our results in a 100-subject group showed that one-lead ECG reached identification rate at 93% accuracy and three-lead ECG acquired 99% accuracy.

1. Introduction

Electrocardiogram (ECG) is a low-cost, noninvasive measure of cardiac electrical activity. ECG analysis has become a standard diagnostic tool for detecting cardiac arrhythmia. Recently, ECG, along with other biometrics like finger and palm prints, has also served as a specific pattern used to recognize individuals. The ECG-based human identification has an advantage in security because it must be acquired from a living body. According to the literature, human identification primarily involves two steps: the ECG features are extracted from ECG waveforms and supervised-learning algorithms are subsequently applied to build classifiers for individual identification in selected groups.

In 2001, Biel et al. [1] demonstrated the feasibility of ECG-based human identification by supervised classification over significant principal components of several morphological features including amplitudes, durations and areas of the P, Q, R, S, T waves and the ST segment. Using 12 features from one lead achieved the same number of correct classifications among 20 persons as well as using 360 (30×12 leads) features.

In some reports only durations of characteristic waves and intervals between characteristic points were selected as discriminant features [2,3]. Kyoso and Uchiyama [2] applied discriminant analysis with two features from P duration, PQ interval, QRS duration and QT interval to identify the registered ECGs from nine subjects by selecting the smallest Mahalanobis distance. Best classification was achieved using the combination of QRS duration and QT interval. Israel et al. [3] extracted 15 time intervals from a heart beat and further reduced feature dimension to 12 by the Wilke's lambda method. Classification by linear discriminate analysis on 29 subjects achieved 81% heart beat recognition rate and 100% individual identification rate.

Shen et al. [4] proposed a two-step identification scheme. A template match method was first applied to find possible candidates. A decision-based neural network with inputs of seven temporal and amplitude features was then used to complete final verification. The experiment on 20 subjects showed 95% successful rate by template matching, 80% by neural network and 100% by combing two methods. In 2006, Shen [5] applied quartile discriminant measurement to reduce the number of ECG features from 17 to 11, thereby achieving an identification rate of 95% for a large population (169 subjects).

Wübbeler et al. [6] proposed a two-dimensional heart vector determined from amplitude values of leads I–III composition. Sum of the squared distances between two heart vectors, their first temporal derivatives, and second derivatives was used to discriminate two ECGs, either from the same or from different subjects.

Most above-mentioned methods are performed by using reduced ECG features or amplitude values based on ECG characteristic points. However, picking up characteristic points is an arduous procedure, particularly in situations of noise contamination and difficult to discern characteristic points. In addition, the reduced features may be insufficient to represent overall characteristics of the ECG, limiting identification performance in a large-population group. Although a high identification rate can be achieved using neural networks [4], the classifier must be rebuilt when a new subject is added, thereby complicating the identification system.

In the present study a novel ECG recognition method is proposed. Instead of extracting the reduced features, the whole ECG signal is quantified in a multi-dimensional phase space. The reconstructed phase space portrait is directly used as a discriminant feature, which not only preserves original characteristics but also takes into account the topological pattern of the ECG. Only R-peak detection is needed for retrieving ECG waveform and the task of detecting P, Q, S and T peaks is avoided. In this paper, two measures are used to quantify the similarity and dissimilarity between ECG phase space portraits. The performance of the proposed identification method was evaluated using an ECG dataset derived from 100 subjects.

* Corresponding author. Tel.: +886 3 2118800x5145; fax: +886 3 2118026.
E-mail addresses: chanhl.net@msa.hinet.net, chanhl@mail.cgu.edu.tw (H.-L. Chan).

0031-3203/$ - see front matter © 2008 Elsevier Ltd. All rights reserved.
doi:10.1016/j.patcog.2008.11.020

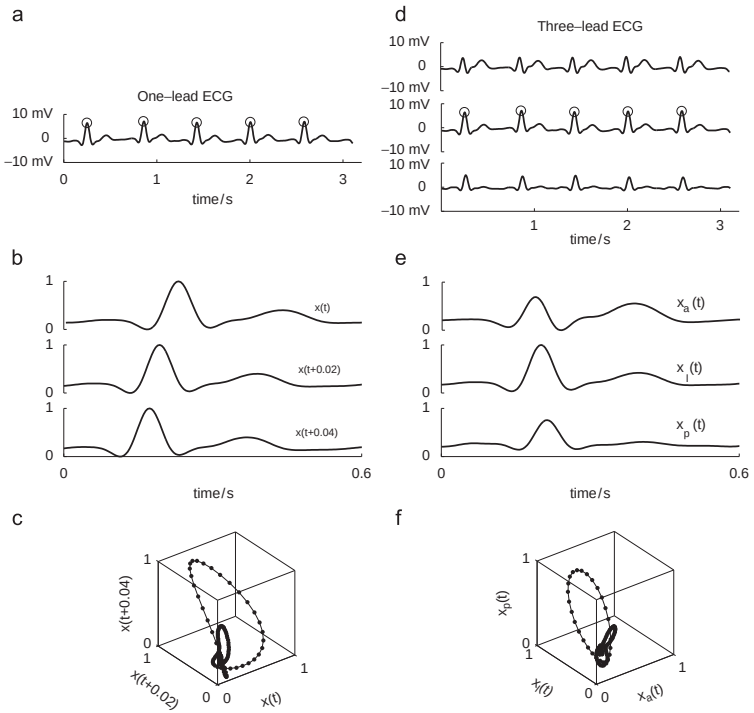

Fig. 1. (a) One-lead ECG. (b) The averaged waveform based on R peaks marked by circles in (a) and its time-delayed waveforms. (c) The reconstructed phase space portrait using the whole ECG waveforms in (b). (d) Three-lead ECG including anterior lead $x_a(t)$, lateral lead $x_l(t)$, and posterior lead $x_p(t)$. (e) Corresponding averaged waveforms. (f) Reconstructed phase space portrait.

2. Methods

2.1. ECG measurement and preprocessing

ECG data were recruited from 100 subjects (37 men and 63 women; mean age 45.6, ranging from 16 to 84 years old) who were examined by routine electroencephalogram in our neurology department. All the examinee sat in an armed chair during the test. Three electrodes were placed: one on the left fifth intercostal space in the mid-clavicular line, one on the horizontal shift to the mid-axillary line, and one on the further horizontal shift to the point between the medial scapula and thoracic spine. The reference electrode was placed on the right subclavicular area. By this arrangement, the anterior, lateral and posterior leads were defined. Two artifact-free ECG epochs of 30 seconds in duration were collected for each subject by a Nicolet EEG machine (The Nicolet, Conshohocken, PA, USA) at a sampling rate of 250 Hz. The first epoch was recorded at the beginning of the test and the second epoch was recorded after 30 minutes with the same electrode locations. All ECG signals were filtered by a fourth-order Butterworth bandpass filter with the passband from 2 to 50 Hz to remove the low-frequency baseline and high-frequency noises. All data processing, including filtering, phase space reconstruction and individual identification was performed using MATLAB 7.4 (The MathWorks, Natick, MA, USA).

2.2. Phase space reconstruction (PSR) of ECG

2.2.1. PSR of one-lead ECG

R-peaks were pointed out from one-lead filtered ECG. As shown in Fig. 1a, the waveforms of five consecutive cardiac cycles were

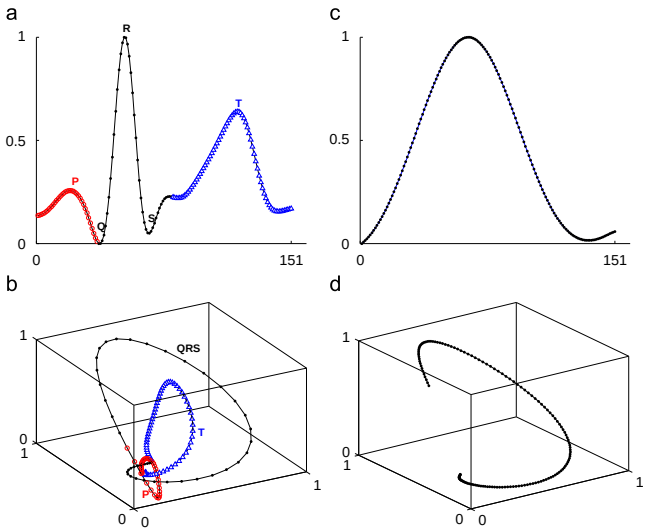

Fig. 2. Left column: if the entire ECG waveform (151 points) is recruited for PSR, there would be one major loop (QRS) and two minor loops (P and T) in the phase space. Right column: if only QRS complex (31 points with five times interpolation) is recruited, there would be only one major loop.

averaged with respect to R peaks. The beat averaging procedure emphasizes ECG characteristics and reduces beat-to-beat waveform variability. The averaged waveform $x_0(t)$ was embedded in a series of three-dimensional vectors with time delay τ:

$$\mathbf{X}_0(t) = [x_0(t)\ x_0(t+\tau)\ x_0(t+2\tau)] \quad (1)$$

The $\mathbf{X}_0(t)$ was normalized to $\mathbf{X}(t)$ (Fig. 1b) so that all values were within the range (0,1):

$$\mathbf{X}(t) = (\mathbf{X}_0(t) - x_{\min})/(x_{\max} - x_{\min}) \quad (2)$$

where $x_{\max}$ and $x_{\min}$ are the maximum and minimum values of $\mathbf{X}_0(t)$. Plotting the normalized vectors over the entire cardiac cycle (Fig. 1b) discloses a phase space portrait (Fig. 1c).

PSR is a multi-dimensional information-preservation method. As shown in Fig. 2, the reflection of P, QRS and T waves are expressed in loop patterns in the phase space (Fig. 2b). Each point in phase space disclose nearby point relationship. In other words PSR can enrich ECG signal. When only QRS complex is recruited, only one compact, major-loop pattern is presented in the phase space (Fig. 2d).

2.2.2. PSR of three-lead ECG

The ECG measured at the anterior, lateral and posterior leads was employed to reconstruct ECG phase space. Similar to PSR of one-lead ECG, the waveforms of five consecutive beats were averaged for each lead and normalized by the extreme values of the three averaged leads. Another series of three-dimensional vectors (Fig. 1e) was defined by

$$\mathbf{X}(t) = [x_a(t)\ x_l(t)\ x_p(t)] \quad (3)$$

where $x_a(t)$, $x_l(t)$ and $x_p(t)$ denote the averaged, normalized ECG of anterior, lateral and posterior leads. As shown in Fig. 1f, PSR from three-lead ECG presents another topological pattern in phase space.

2.3. Portrait comparison methods

Fig. 3 shows the phase space portraits derived from only QRS complexes of the first and second epochs in the same person (intra-comparison) and from the first epochs of two persons (inter-comparison). The spatial correlation (SC) and mutual nearest point distance (MNPD) were used to quantify similarity and dissimilarity, respectively, between ECG phase space portraits.

2.3.1. Spatial correlation

Due to amplitude normalization, each ECG portrait was distributed over a normalized phase space with a range of (0,1) on each axis. In order to measure overlapping between two portraits in phase space, the normalized phase space was first divided into $M \times M \times M$ equal-size cubes. The ECG portrait was then transformed to a histogram-based nonparametric distribution, termed by $N(i,j,k)$, $1 \leqslant i,j,k \leqslant M$, recording the number of portrait points in each cube. Fig. 2 shows the derived histograms (middle row) from respective ECG portrait (upper row) according to 10×10×10 partitions. The similarity between portraits $\mathbf{X}(t)$ and $\mathbf{Y}(t)$ is quantified by the SC based on the cube-density histograms, which is defined by

$$SC(\mathbf{X},\mathbf{Y}) = \frac{\sum_{1 \leqslant i,j,k \leqslant M} N_{\mathbf{X}}(i,j,k) \times N_{\mathbf{Y}}(i,j,k)}{M^3 - 1} \quad (4)$$

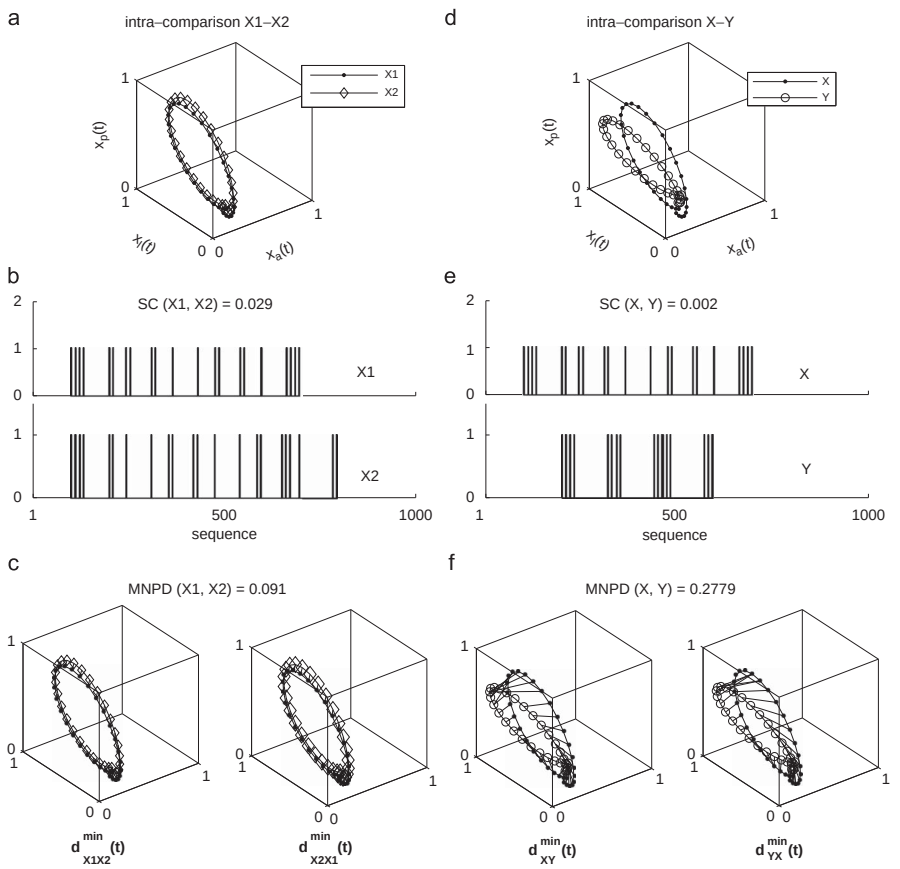

Fig. 3. (a) Reconstructed phase space portrait using QRS complex, intra-individual comparison of portraits $\mathbf{X}_1$ and $\mathbf{X}_2$ of different epochs from the same person. (b) Corresponding cube-density histograms over 10×10×10 partitioned cubes, sequencing from 1 to 1000; SC, spatial correlation between two histograms. (c) Mutual nearest point distance (MNPD) computed based on point-to-nearest-point distances from $\mathbf{X}_1$ to $\mathbf{X}_2$ and from $\mathbf{X}_2$ to $\mathbf{X}_1$. (d–f) Inter-individual comparison of portraits $\mathbf{X}$ and $\mathbf{Y}$ recruited from different persons; the others same as intra-individual comparison.

If two comparing portraits are similar in trajectory, the accumulation of the product of $N(i,j,k)$ at the same position will gain more; vice versa. The denominator M^3-1 is used to normalize the index by the freedom of cubic number. As shown in Fig. 3, the SC of the intra-individual pair ($\mathbf{X}_1$ and $\mathbf{X}_2$) is greater than that of the inter-individual pair ($\mathbf{X}$ and $\mathbf{Y}$) due to a higher portrait similarity.

2.3.2. Mutual nearest point distance

A novel measure based on directly calculating point-to-nearest-point distances was used to quantify dissimilarity between two ECG portraits. Given two portraits $\mathbf{X}(t)$ and $\mathbf{Y}(t)$ of identical P points where $t = t_1 \ldots t_P$, their MNPD was computed in a bidirectional way:

$$MNPD(\mathbf{X},\mathbf{Y}) = \frac{\sum_{t=t_1}^{t_P} d_{\mathbf{XY}}^{\min}(t) + \sum_{t=t_1}^{t_P} d_{\mathbf{YX}}^{\min}(t)}{2 \times P} \quad (5)$$

MNPD is a measure of portrait distance in phase space. Inspecting from portraits $\mathbf{X}$ to $\mathbf{Y}$, the $\mathbf{X}$-to-$\mathbf{Y}$ portrait distance is defined by the sum of nearest distance $d_{\mathbf{XY}}^{\min}$ from every point in $\mathbf{X}$ to $\mathbf{Y}$ (Fig. 4a). Similarly, the point-to-nearest-point distances from $\mathbf{Y}$ to $\mathbf{X}$, $d_{\mathbf{YX}}^{\min}$ are derived and summed together. Inspecting in mutual direction (from $\mathbf{X}$ to $\mathbf{Y}$ and from $\mathbf{Y}$ to $\mathbf{X}$) is indicated in avoidance of the extreme condition (Fig. 4b) that also gives a small $\mathbf{X}$-to-$\mathbf{Y}$ portrait distance

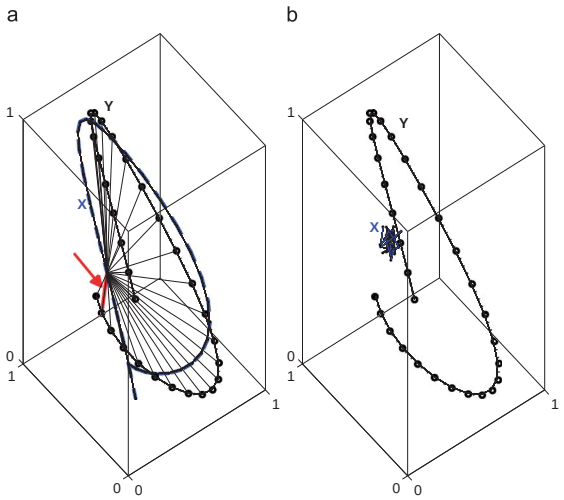

Fig. 4. (a) The **X**-to-**Y** portrait distance is defined by the sum of nearest distance from every point in **X** to Y. The arrow shows the nearest distance for a point in **X** to **Y**. (b) An extreme condition that gives a small **X**-to-**Y** portrait distance though **X** and **Y** are quite different, which is avoidable by mutual calculation of **X**-to-**Y** and **Y**-to-**X** portrait distance.

though **X** and **Y** are quite different. The denominator $2\times P$ is to normalize the index by the freedom of point number. As shown in Fig. 3, the MNPD of the intra-individual pair ($\mathbf{X}_1$ and $\mathbf{X}_2$) is smaller than that of the inter-individual pair (**X** and **Y**).

2.3.3. Computational complexity

The computational demands for computing SC and MNPD were analyzed by counting the required operations including comparison, addition, multiplication, division, and square-root operations. Although these operations may have different execution cycles in different machines, the cost for each operation was expressed by one floating-point operation (FLOP) for simplicity. For the SC computation, a P-point ECG waveform requires $3\times P$ multiplications to determine the locations of their belonging cubes and P additions to counting cube density. Computing the SC of two cube-density histograms (Eq. (4)) requires M^3 multiplications, M^3 additions, and one division. The total number of FLOPs is $8\times P+2\times M^3+1$. For a 151-point SC $10\times10\times10$ computation ($P=151$ and $M=10$), it requires 3209 FLOPs.

For the MNPD, each point-to-point distance requires three multiplications, two additions, and one square-root operation (six FLOPs). Given a point in **X** portrait, it requires P point-to-point distance calculation and P comparison to find $d_{\mathbf{XY}}^{\min}$ ($7\times P$ FLOPs). Calculating $\sum d_{\mathbf{XY}}^{\min}$ requires $7\times P^2+P$ FLOPs. The total FLOPs to compute MNPD (Eq. (5)) is $14\times P^2+2\times P+2$. For a 151-point MNPD computation ($P=151$), it requires 319 518 FLOPs.

2.4. Individual identification based on portrait comparing indexes

A match decision is made if the SC (MNPD) value is higher (or lower) than the threshold which is set. To find the cutoff threshold for the SC (or MNPD)-based identification in our experiment of 100 subjects, a comparison matrix with a size of 100 (from reference)×100 (from test) was used to record the computed SC (or MNPD). The diagonal elements store the intra-individual SC (or MNPD) between two epochs recorded at different times in each person. The remaining elements store the inter-individual SC (or MNPD) between possible pair of subjects. Based on the comparison matrix, the sets of sensitivity, specificity, and accuracy of individual identification using various cutoff thresholds step-by-step, from low-end to high-end, were computed. Sensitivity was defined as the ratio of intra-individual SC (or MNPD) that was also higher (or lower) than the selected cutoff threshold (correct identification in the intra-individual comparisons). Specificity was defined as the ratio of inter-individual SC (or MNPD) that was also lower (or higher) than the selected cutoff threshold (correct discrimination in the inter-individual comparisons). Accuracy was equal to the mean of sensitivity and specificity. The optimal cutoff threshold was set to the value that provided the highest accuracy.

In addition, individual is also identified by the combination of simultaneous measures of SC and MNPD in "OR" pattern (MNPD ∪ SC), defining match if any, or in "AND" pattern (MNPD ∩ SC), defining match if both.

2.4.1. Performance evaluation

We tested various configurations for optimal performance. The input channel can be one-lead (anterior, lateral or posterior) or three-lead ECG. The input signal length can be 31 points (0.12 seconds) R-centered short segment containing the ORS complex or 151 points (0.6 seconds) R-centered long segment covering the P, QRS and T waves. In addition another two segments were created from the short one with five- or 10-times finer resolution by cubic interpolation in order to increase the density of the reconstructed phase–space portraits. The embedding lag for three-dimensional PSR from one-lead ECG was investigated with 0.004, 0.012, 0.02, 0.028 or 0.04 seconds. The identification methods MNPD, SC with axis separation 6, 10 or 14 partitions were used. In each configuration the optimal performance was set by highest accuracy.

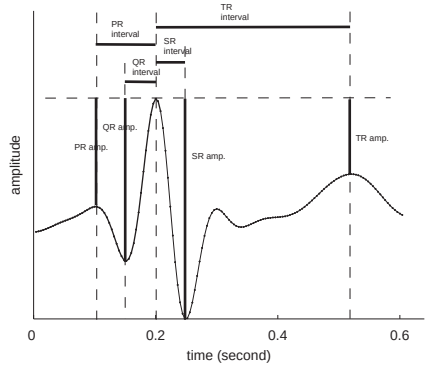

Fig. 5. Eight ECG features (amplitudes and intervals of PR, QR, SR and TR) are extracted from P, Q, R, S and T characteristic points in a five-beat averaged ECG waveform.

2.5. Characteristic-point comparison methods

2.5.1. Feature extraction

To compare our method with commonly used methods based on reduced ECG features, characteristic points P, Q, R, S and T were pick up from 5-beat averaged waveform for each lead. Eight features, including time intervals of PR, QR, SR and TR and amplitude differences of PR, QR, SR and TR, were extracted (Fig. 5). For each subject 1-channel ECG input acquired eight features and 3-channel ECG input acquired 24 features. In addition, principal component analysis was applied to the ECG features derived from these 100 subjects. The first four principal components for 1-channel ECG and first nine principal components for 3-channel ECG, reaching 99% of total variance, were also used as discriminant features.

2.5.2. Neural network-based classifiers

The extracted ECG features or their significant principal components were respectively used as discriminant features. Two types of neural networks were investigated. The first-type classifier was constructed by backpropagation neural network with 20 or 30 hidden neurons and 100 output nodes for all 100 subjects. The ECG features derived from the first epochs of all subjects were served as a training set. The desired output was set 1 for target and −1 for non-target. The network training was performed by the Levenberg–Marquardt direction rule. The ECG features derived from the second epochs were used as a test set. The test data was set "true" if the network output exceeded a cutoff threshold; vice versa. The performance was evaluated by the same concept mentioned in Section 2.4. Optimal cutoff threshold was determined with highest accuracy. The second-type classifier was constructed through radial basis function neural network with spread constant 1 or 10. The training, test sets and performance evaluation were similar to those employed in backpropagation neural network.

2.5.3. Point distance-based classifier

The ECG features, as those inputs for neural networks, were normalized to a range of (0,1) according to the 100 subjects, then were projected to a point in multi-dimensional space. The performance was evaluated based on a comparison matrix indicating Euclidean distances (point distances) between test points and training points. Similar to the MNPD, a match decision was made if the point distance was lower than a cutoff threshold. The optimal threshold was set to the value that provided the highest accuracy.

3. Results

The computation time is demonstrated by the comparisons based on 3-lead, 151-point ECG samples. The time for deriving the elements in the upper triangular of the 100×100 comparison matrix (Section 2.4) was 15.1 seconds by the SC method and 413.9 seconds by the MNPD method that were executed on the Matlab 7.4 in a personal computer (Intel Core 2 Duo 3.2-GHz CPU, 2-GB RAM). The MNPD method took more computation time than the SC method as well as the theoretical analysis.

Fig. 6 shows the histograms of intra-individual (middle panel) and inter-individual (lower panel) MNPD derived from three-lead 31-point ECG of 100 subjects. When a lower threshold was adopted, more intra-individual MNPDs cannot be recognized as from the same subject, decreasing identification sensitivity. When a higher threshold was adopted, more inter-individual MNPDs cannot indicate portraits' distinction, decreasing identification specificity. By migrating threshold from low end to high end we can observe the trend of sensitivity and specificity versus the selected threshold in Fig. 6 (upper panel). The optimal threshold is set to the value with highest accuracy, defined as the mean of sensitivity and specificity. In this case, optimal threshold was set to 0.141 where acquired 99% sensitivity and 98% specificity.

In our experiments for 1-channel ECG configurations, anterior lead, 31-point short segment with five times interpolation and 0.02 seconds time delay acquired optimal performance. For three-channel ECG configuration 31-point short segment with five times interpolation acquired better performance than that without finer interpolation. The SC method with 10 axis partitions acquired highest accuracy than those with 6 or 14 axis partitions.

Table 1 lists individual identification performance using the optimal configurations in portrait comparison methods. Use of three-lead ECG resulted in better identification rates than one-lead ECG. The MNPD-based method generally had better identification performance than the SC-based method. In the SC-based identification, using only QRS complex (31 points with five times interpolation) to reconstruct phase space gained significant better performance than using the entire cardiac-cycle waveform (151 points).

Table 2 shows the correlation coefficients for the SC and MNPD among 100 subjects. The SC and MNPD had moderately negative correlation. The correlation was weaker in three-lead ECG than in one-lead ECG. In inspecting simultaneous measures of SC and MNPD, specificity increased in "OR" pattern (MNPD ∪ SC), and sensitivity increased in "AND" pattern (MNPD ∩ SC); however, without improvement in overall accuracy.

Table 3 lists individual identification performance incorporated with neural networks and point-distance methods based on the extracted ECG features or their significant principal components. In our experiment backpropagation neural network with 20 hidden neurons had similar performance as using 30 hidden neurons, so 20 hidden neurons were adopted. Radial basis function neural network with spread constant 10 had better performance than using spread constant 1, so spread constant 10 was adopted. More detailed input acquired from three-lead ECG resulted in better identification performance than one-lead ECG. Using principal components did not improve identification rate. Point-distance comparison methods acquired the best identification rates, particularly in three-lead ECG that reached 100% sensitivity and 95% specificity. Radial basis function neural network had a little better identification rate than backpropagation neural network.

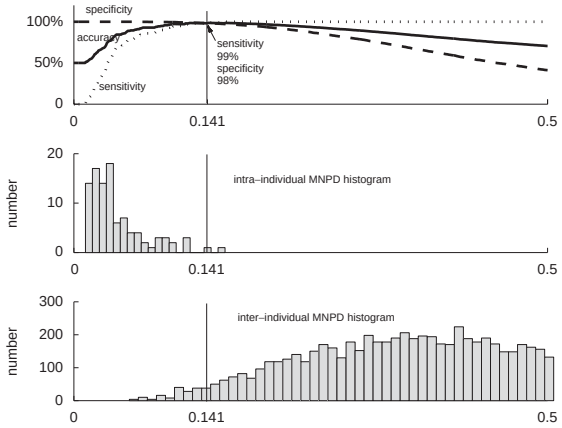

Fig. 6. The histogram of intra-individual (middle panel) and inter-individual (lower panel) mutual nearest point distance (MNPD) based on three-lead 31-point ECG derived from the enrolled 100 subjects. Upper panel: sensitivity, specificity, and accuracy of individual identification based on various cutoff thresholds. Sensitivity was defined as the number of intra-individual MNPD that was also lower than the selected cutoff threshold divided by the number of intra-individual MNPD. Specificity was defined as the number of inter-individual MNPD that was also higher than the selected cutoff threshold divided by the number of inter-individual MNPD. Accuracy was equal to the mean of sensitivity and specificity.

Table 1
Classification performance on various configurations in portrait comparison methods.

ECG leads	ECG points	Comparison method	Sensitivity (%)	Specificity (%)	Accuracy (%)
1	31	MNPD	98	88	93
1	151	MNPD	95	89	92
3	31	MNPD	99	98	99
3	151	MNPD	98	95	97
1	31	SC 10	96	87	92
1	151	SC 10	89	75	82
3	31	SC 10	97	96	97
3	151	SC 10	98	86	91

Spatial correlations SC 10 computed upon 10×10×10 phase space partitions; MNPD: mutual nearest point distance. Sensitivity, specificity and accuracy were defined as Fig. 6.

Table 2
Correlation coefficients for SC and MNPD.

ECG leads	ECG points	Correlation coefficient
1	31	−0.7861
1	151	−0.6162
3	31	−0.5541
3	151	−0.5718

Correlation coefficients were computed based on the comparison matrices described in Section 2.4.

Table 3
Classification performance on various configurations in characteristic-point comparison methods.

ECG leads	ECG features	Comparison method	Sensitivity (%)	Specificity (%)	Accuracy (%)
1	8/4*	BP20	89/95	86/67	87/81
3	24/9*	BP20	95/94	95/86	95/90
1	8/4*	RB10	86/74	91/81	89/77
3	24/9*	RB10	97/100	98/93	98/96
1	8/4*	PD	93/93	93/93	93/93
3	24/9*	PD	100/100	95/95	98/98

For 1-channel anterior-lead ECG, input with eight extracted features or four major principal components (4*). For 3-channel ECG, input with 24 extracted features or nine major principal components (9*). BP 20: backpropagation with 20 hidden neurons; RB10: radial basis function with spread constant 10; PD: point distance in multi-dimensional space. Sensitivity, specificity and accuracy were defined as Fig. 6.

4. Discussion

Most ECG-based human identification methods rely on one-to-group comparison. The input feature is sent to a group classifier based upon the features of all subjects in the group. In our experiment the neural network did not perform as well as expected, probably due to training limit for a large sample. Another disadvantage is the classifier must be retrained when a new person is added to the group. On the contrary, our proposed identification method is performed on the basis of one-to-one comparison. The class is matched by inspecting similarity (SC) or dissimilarity (MNPD) between the input portrait and compared portrait. If the comparing measure meets the match criterion, a true identification is achieved. In addition, a new class can be created by directly inserting the new portrait into the identification system.

A template match based on raw ECG waveforms is a direct method for individual identification. Matched by the extracted features from ECG characteristic points is the commonly used method in literatures. Incorporating with a point distance-based classifier gained good identification rate as well as the PSR-based method in our experiment. However, the main difficulty comes from arduous and imprecise ECG characteristic point detection. The proposed method is actually a refined template match method with several advantages. Only R-point needs to be picked out for the input portrait. Phase space normalization allows the ECG morphology to be amplitude-free and direct comparison to be feasible. The PSR can enrich feature information by adding nearby-space (three-lead ECG) or nearby-point (one-lead ECG) relationships. Portrait comparison using the SC or the MNPD can avoid waveform alignment.

In this paper the SC and MNPD methods are applied to compare ECG portraits. The SC quantifies portraits' overlap in phase space by cross correlation of discrete cubic densities. Using only QRS complex has a better identification rate than using the entire cardiac-cycle waveform. The QRS complex is sparsely distributed in the phase space while low-amplitude components including P- and T-waves are more concentrated in phase space, producing higher cubic density than the QRS complex. The product of higher cubic densities dominates the SC computation while the contribution from the QRS complex is comparably small. The MNPD can improve identification performance by using more precise point-to-nearest-point distances rather than cubic densities between portraits.

In 1998, Sörnmo [7] proposed a vectocardiographic loop alignment to quantify morphological variability, including loop angle rotation and scaling factor, which was proposed to detect respiratory-induced movements of the heart. The Sörnmo method is based on the assumption of similar topologies in beat-to-beat vectocardiographic loops. On the contrary, individual identification relies on different morphological patterns between persons. In the circumstance of different portrait morphology, by mutual accumulation of nearest point–point distance between two portraits, our MNPD method becomes the most intuitive and reasonable solution for quantifying such morphological differences.

In practical application of human identity recognition by ECG, we would suggest one-to-one comparisons combined with a code that is initially input. The input code not only raises the security level of the identification system, but also can be used as a reference code to aggregate the matched ECG into its own cluster. Next time the ECG cluster belonging to an individual is picked out from the databank by the input code, the test ECG will be compared to the representative pattern of the cluster.

In conclusion, PSR-based ECG input helps in automated measure, avoiding imprecise characteristic point identification. The PSR portrait contains all ECG points and makes use of nearby-point relationship to enrich feature information. Our proposed portrait comparison methods are one-to-one refined template match without the need for supervised training. Using one-lead ECG provides fast and good comparison performance. Excellent performance is achieved by using three-lead ECG due to the existence of more spatial information.

References

[1] L. Biel, O. Pettersson, L. Philipson, P. Wide, ECG analysis: a new approach in human identification, IEEE Trans. Instrum. Meas. 50 (2001) 808–812.
[2] M. Kyoso, A. Uchiyama, Development of an ECG identification system, in: Proceedings of the 23rd Annual International Conference of IEEE EMBS, 2001, pp. 3722–3723.
[3] S.A. Israela, J.M. Irvineb, A. Chengb, M.D. Wiederholdc, B.K. Wiederholdd, ECG to identify individuals, Pattern Recognition 38 (2005) 133–142.
[4] T.W. Shen, W.J. Tompkins, Y.H. Hu, One-lead ECG for identity verification, in: Proceedings of the 24th Annual International Conference of IEEE EMBS, 2002, pp. 62–63.
[5] T.W. Shen, Quartile discriminant measurement (QDM) method for ECG biometric feature selection, in: Proceedings of International Symposium of Biomedical Engineering, Taiwan, 2006, no. 10394.
[6] G. Wübbeler, M. Stavridis, D. Kreiseler, R.D. Bousseljot, C. Elster, Verification of humans using the electrocardiogram, Pattern Recognition Lett. 28 (2007) 1172–1175.
[7] L. Sörnmo, Vectocardiographic loop alignment and morphologic beat-to-beat variability, IEEE Trans. Biomed. Eng. 45 (1998) 1401–1413.

About the Author—SHIH-CHIN FANG received the M.D. degree from National Taiwan University, Taiwan, in 1996. He joined the Department of Neurology, Cardinal Tien Hospital Yung Ho Branch, Taipei, Taiwan, since 2004. He is currently pursuing the Ph.D. degree at the Department of Electrical Engineering, Chang Gung University, Taiwan. His research interests include clinical neurology and nonlinear analyses of biomedical signals.

About the Author—HSIAO-LUNG CHAN received the Ph.D. degree from the Department of Electrical Engineering from the National Taiwan University, Taipei, Taiwan, in 1997. He is currently an Associate Professor at the Department of Electrical Engineering, Chang Gung University, Taoyuan, Taiwan. His research interests include cardiovascular and electrophysiological information processing and embedded system design for medical instrumentation.